Changes toward Earlier Streamflow Timing across Western North America

IRIS T. STEWART

Scripps Institution of Oceanography, La Jolla, California

DANIEL R. CAYAN

Scripps Institution of Oceanography, and U.S. Geological Survey, La Jolla, California

MICHAEL D. DETTINGER

U.S. Geological Survey, and Scripps Institution of Oceanography, La Jolla, California

(Manuscript received 2 January 2004, in final form 9 July 2004)

ABSTRACT

The highly variable timing of streamflow in snowmelt-dominated basins across western North America is an important consequence, and indicator, of climate fluctuations. Changes in the timing of snowmelt-derived streamflow from 1948 to 2002 were investigated in a network of 302 western North America gauges by examining the center of mass for flow, spring pulse onset dates, and seasonal fractional flows through trend and principal component analyses. Statistical analysis of the streamflow timing measures with Pacific climate indicators identified local and key large-scale processes that govern the regionally coherent parts of the changes and their relative importance.

Widespread and regionally coherent trends toward earlier onsets of springtime snowmelt and streamflow have taken place across most of western North America, affecting an area that is much larger than previously recognized. These timing changes have resulted in increasing fractions of annual flow occurring earlier in the water year by 1–4 weeks. The immediate (or proximal) forcings for the spatially coherent parts of the year-to-year fluctuations and longer-term trends of streamflow timing have been higher winter and spring temperatures. Although these temperature changes are partly controlled by the decadal-scale Pacific climate mode [Pacific decadal oscillation (PDO)], a separate and significant part of the variance is associated with a springtime warming trend that spans the PDO phases.

1. Introduction

The loss of mountain snow accumulation and reductions in snowmelt-derived water supply are among the primary consequences expected from climate warming. Thus it is with some concern that a shift toward earlier spring snowmelt-derived streamflow, starting in the late 1940s, has been observed for several regions across western North America (Roos 1987, 1991; Wahl 1992; Aguado et al. 1992; Pupacko 1993; Dettinger and Cayan 1995; Cayan et al. 2001; Stewart et al. 2004; Regonda et al. 2005). Spring streamflow during the last five decades has shifted so that the major April–July streamflow peak now arrives one or more weeks earlier, resulting in declining fractions of spring and early summer river discharge. Importantly, as yet, there has been little concurrent change in the total annual discharge (Wahl 1992; Aguado et al. 1992; Dettinger and Cayan 1995) and only spotty evidence for decreasing April–June streamflow volumes (Wahl 1992). Climatic factors affect the timing and amount of discharge in river basins, introducing significant spatial and temporal variability as well as regional coherence (see Cayan et al. 2001). The regional coherence in the observed changes for snowmelt-dominated basins strongly suggests that climate changes and, in particular, temperature, are playing a dominant role, as moderate temperature changes mostly affect midelevation snowmelt-dominated basins most susceptible to melting (i.e., Mote 2003a).

Concurrent with the observed snowmelt and streamflow timing trends, the average annual temperature have increased 1°–2°C since the 1940s over the (north) western part of North America, especially during the winter and spring seasons (Karl et al. 1993; Lettenmaier et al. 1994; Dettinger and Cayan 1995; Vincent et al. 1999), while precipitation trends are neither as mono-

Corresponding author address: Dr. Iris Stewart, Scripps Institution of Oceanography, 9500 Gilman Drive, La Jolla, CA 92093–0224.
E-mail: istewart@ucsd.edu

tonic, large (relative to variability), nor widespread, as the temperature trends. Tree ring record-based temperature reconstructions suggest that spring temperatures over western North America in the last 50 years are higher than during any equivalent period in the last 900 years (Luckman et al. 1997; Luckman 1998; Jones et al. 2001). These findings are consistent with the retreat of snow cover extent and glaciers across much of the Northern Hemisphere (Walters and Meier 1989; Hodge et al. 1998; Luckman 1998; McCabe and Fountain 1995; Groisman et al. 1994; Bitz and Battisti 1999; McCabe et al. 2000). In addition to these temperature changes, an increase in annual precipitation over Canada and the contiguous United States over the last decades has been identified (Karl et al. 1993; Groisman and Easterling 1994). Previous studies have linked streamflow timing trends with large-scale temperature patterns (Aguado et al. 1992; Dettinger and Cayan 1995) and bioclimatic signals (Cayan et al. 2001). The sensitivity of streamflow timing to temperature has been investigated by studies linking general circulation models to hydrologic streamflow models in the west, especially for rivers in the Sierra Nevada (Gleick 1987; Lettenmaier and Gan 1990; B. J. Tsuang and J. A. Dracup 1991, personal communication; Jeton et al. 1996; Hamlet and Lettenmaier 1999; Miller et al. 1999; Kim 2001; Snyder et al. 2002; Dettinger et al. 2004; Stewart et al. 2004). While these previous studies indicate that temperature increases would produce earlier streamflow, they generally have not implicated precipitation in causing streamflow timing variations and shifts, with the exception of the study by Hamlet and Lettenmaier (1999). Although it is beyond the investigation of this study, it should be recognized that the warming trends responsible for the observed streamflow timing changes are likely to affect precipitation and further hasten streamflow timing. Winter and spring warming causes an increased fraction of the precipitation to come as rain, resulting in a reduced snowpack and an even earlier melt. Furthermore, even in the absence of warmer temperatures, glacial melt can have unexpected inputs and effects on streamflow and streamflow timing (Fountain and Tangborn 1985). Increased glacial melting from warming may exacerbate the effects of glacial melt on streamflow (timing), thus eliciting different responses from glacial and nonglacial basins to climatic changes.

The observed hydroclimatic shift is quite certainly linked to decadal fluctuations of the winter and spring atmospheric circulation over the North Pacific Ocean and North America (Dettinger and Cayan 1995). In particular, since the late 1970s, there has been strong El Niño–Southern Oscillation (ENSO) activity (Trenberth 1996), and the Pacific Decadal Oscillation (PDO) (Mantua et al. 1997) shifted from its warm to its cool phase in 1947, and back to its warm phase in 1976. Recent observations during the 1999–2002 period suggest that the PDO may have reentered another cool phase (more information available online at http://tao.atmos.washington.edu/pdo/). Although the PDO (and ENSO) have clearly contributed to changing temperatures in the West, it is still uncertain whether the observed temperature and snowmelt-derived streamflow timing trends are predominantly a symptom of natural climate variability (such as the PDO) or arise from a different mechanism, such as an early signal of human-induced global change and its associated temperature increases. Even if the observed temperature and streamflow timing trends were eventually shown not to be associated with global warming, regional-to-continental-scale analysis of streamflow data, such as the one presented here, might provide an observational analog to potential global change impacts.

Thus we seek 1) to map the presence, magnitude, and spatial extent of streamflow timing changes; 2) to identify the proximal processes that govern the regionally coherent patterns of timing change; and 3) to resolve their climatic causes. These issues are addressed through a comprehensive statistical analysis of streamflow records from Alaska, western Canada, and the western conterminous United States, a larger region than has been examined previously. A trend analysis is conducted to determine the presence and magnitude, as well as spatial boundaries, of the changes in streamflow timing. Patterns of regionally coherent variation are identified through principal component analysis (PCA). The relationship of streamflow timing changes to climate fluctuations and changes is explored by correlating timings with temperature, precipitation, and Pacific climate indicators, such as atmospheric circulation, ENSO, and PDO. Because the PDO index is not necessarily independent of the global warming trend observed over the past five decades, the leading principal components (PCs) of streamflow timing changes are also compared to global sea surface temperatures (GSSTs), in an attempt to determine the relative importance of each of these climate influences. In addition, statistical and correlation analyses were employed to distinguish the relative impact of decadal-scale climate variability on regionally coherent streamflow timing changes as compared to that due to long-term climatic trends.

2. Data

Streamflow timing and amounts for this study are calculated from streamflow records for western North American watersheds located north of 30°N latitude and west of 105°W longitude. The streamflow records for the U.S. portion of the study area were selected from the U.S. Geological Survey (USGS) Hydro-Climatic Data Network (HCDN) (Slack and Landwehr 1992). The HCDN dataset contains daily streamflow observations from U.S. Geological Survey stream gauges that are considered to be relatively unaffected by anthropogenic influences, land-use changes, mea-

surement changes, and measurement errors. Monthly streamflow for the Canadian portion was obtained from Environment Canada. As some streamflow records begin as early as 1901, but most do not commence until several decades later, the bulk of the analyses are performed for the 1948–2002 period.

Only snowmelt-dominated gauges with more than 30 complete years of record since 1948 were used for most of the analyses in this study. A stream from the HCDN data was defined as snowmelt dominated if a snowmelt pulse marking the onset of very rapid snowmelt could be identified by methods described in Cayan et al. (2001) and those described below for more than 30% of the available yearly records in the study period; 332 of the 356 U.S. and 53 of the 132 Canadian gauges satisfied the minimum record-length requirement. Of the 332 U.S. gauges, 241 satisfied the snowmelt criteria. All Canadian streams were assumed to be snowmelt dominated. Overall, then, 294 gauges were retained as snowmelt-driven streamflow records. Additionally, another 91 non-snowmelt-dominated gauges were employed for comparative purposes. The annual hydrographs for the rivers analyzed here share some common characteristics. In general, they are dominated by spring and early summer snowmelt-derived streamflow for snowmelt-dominated rivers and by winter precipitation for non-snowmelt-dominated rivers. Low streamflow volumes usually prevail in late summer and fall. In the snowmelt-dominated basins, winter low flows quickly give way to high flows with the beginning of the spring snowmelt. The timing of the spring transition period is a function of interdependent factors, such as altitude, latitude, aspect, vegetation, temperature, and the type, amount, and temporal distribution of precipitation.

Temperature and precipitation data were drawn from two sources. All correlation and trend analyses used the time series of gridded average monthly temperature and precipitation anomalies from Eischeid et al. (1995). Temperature (°C) and precipitation (mm) were anomalized (expressed as departures from long-term means) with respect to the 1951–80 climatological period. The Eischeid data are available on a 5° × 5° grid starting in 1851 and was initially used to test for climate-driven streamflow timing changes in the pre-1948 period. For the composite analyses, temperature and precipitation are taken from the monthly "divisional" data compiled by the National Climatic Data Center (NCDC) for the conterminous United States for the 1948–2002 period. The temperature and precipitation data are area averages for quasi-uniform climate districts that usually contain several stations.

Snow-water equivalent (SWE) for a set of snow courses in the western United States and western Canada were obtained from the U.S. Department of Agriculture Natural Resources Conservation Service and from the California Department of Water Resources Cooperative Snow Surveys Program. Observations are made on approximately the first day of each month between January and May and usually reach their seasonal apex on 1 April (Cayan 1996).

Seasonal mean Northern Hemisphere atmospheric circulation anomalies are represented here by the 700-mb pressure-level heights (Namias 1979) from the National Oceanic and Atmospheric Administration (NOAA)/National Centers for Environmental Prediction (NCEP 2003). The 700-mb heights analyzed are seasonal averages on a 5° latitudinal × 10° longitudinal diamond grid over the 1948–2002 period.

Decadal-scale variability over the North Pacific region is characterized by a PDO index, defined as the leading principal component of North Pacific monthly sea surface temperature (SST) variations, north of 20°N (Mantua et al. 1997). The ENSO status is given here by a yearly Southern Oscillation index (SOI), using monthly data, which are based on the standardized Tahiti–Darwin sea level pressure anomalies from NCEP (2003). A measure of global average ocean temperatures (GSSTs) are a global average of the combined International Comprehensive Ocean–Atmosphere Data Set (I-COADS) and NCEP SST anomalies with respect to their 1950–79 climatology. Since SST in the Pacific has varied differently in winter and spring, the effect of the seasonality of the PDO on its relationship to streamflow timing was assessed through correlations with seasonal [December–February (DJF), March–May (MAM), June–August (JJA), October–April (OA), and water year (1 October of the previous year to 30 September)] PDO indices. Because the OA index resulted in the highest and most widespread correlations with streamflow timing, the PDO, SOI, and GSST indices for analyses conducted here employed OA average values.

3. Methods

The study domain included watersheds in the western 11 mountainous states of the conterminous United States, the five western Canadian provinces, and Alaska. Streamflow timing trends were analyzed in terms of three measures.

1) Monthly and seasonal fractional flows, defined as the ratio of the streamflow that takes place in a given month or season to the total streamflow in the water year. The snowmelt season fractional flow was defined as the ratio of the streamflow that occurs during the April through July (AMJJ) period to the total water year.
2) The date of the beginning of the spring or early summer snowmelt-derived streamflow for snowmelt-dominated rivers ("spring pulse onset").
3) The date marking the timing of the center of mass of annual flow center timing (CT) for each water year.

Each of the measures were examined for the presence of linear trends for the period from 1948 to 2002. The 1948–2002 period proved to be the time segment

with the most robust trends in the 1901–2002 period (analysis not shown). This period is consistent with the time frame of temperature and streamflow timing changes previously reported (Wahl 1992; Dettinger and Cayan 1995; Cayan et al. 2001) and provided the most complete (spatially and serially) data coverage. In this analysis, the statistical significance of the trends was determined through t and F tests. Trends in monthly fractional flows for each gauge were used to identify changes in the distribution of flow throughout the water year, while those of AMJJ fractional flows determined the changes in the relative importance of streamflow during the time of snowmelt from a seasonal perspective. The AMJJ and monthly fractional flows were determined for all 294 snowmelt and the additional 91 non-snowmelt-dominated streams.

The existence and the date of the spring pulse onset for the daily HCDN gauge records were determined by an algorithm developed by Cayan et al. (2001, their Fig. 3). The algorithm estimates the onset of the spring snowmelt pulse by identifying the day on which the cumulative departure from the mean flow is minimum. Here the mean flow for calendar days 9–248 was used. This analysis assumes that the beginning of the snowmelt-derived streamflow pulse signal for a particular stream in a given year was correctly identified by the algorithm if 1) more than 200 daily records were available to determine the mean flow and 2) their calculated day of minimum cumulative departure fell between 15 February and 15 August. The spring pulse onset could not be determined for Canadian gauges because daily streamflow data were not available.

The timing of the center of mass of the annual flow (CT) was calculated from

$$\mathrm{CT} = \Sigma(t_i q_i)/\Sigma q_i, \tag{1}$$

where t_i is time in months (or days) from the beginning of the water year (1 October), and q_i is the corresponding streamflow for month i (or water yearday, i). The two timing measures, spring pulse onset and CT, are illustrated in Fig. 1 by two daily average flow hydrographs of the Carson River, California, one each for earlier (1952) and later (1996) in the study period. Although total streamflow in the two years was approximately equal, the start of the snowmelt occurred about 2–3 weeks earlier in 1996 than in 1952. The earlier snowmelt in 1996 resulted in a decrease in late season streamflow and a prolonged summer drought period. Figure 1 illustrates that the start day of the snowmelt pulse (i.e., the time when snowmelt streamflow starts to "take off") often cannot be accurately determined, even by the automated procedure used, due to the presence of smaller streamflow peaks that represent false starts to the primary spring snowmelt period. As changes in CT alone are not necessarily related to the timing of snowmelt, the trends toward earlier snowmelt pulse onset dates are presented as evidence for observed earlier actual melting. Since the snowmelt runoff pulse is by far the largest contribution to annual flow for snowmelt-dominated basins in the West, CT provides a time-integrated perspective of the timing of this pulse and the overall distribution of flow for each year, and it is less noisy than the spring pulse onset date. Thus, most results are presented here in terms of the CT measure. The CT and spring pulse onset date are positively correlated (r = 0.5–0.8 for most gauges) and significantly correlated for 74% of the gauges.

The relationship between streamflow timing for individual gauges and regional climate was established through correlation analysis of CT with a temperature index (TI) and a precipitation index (PI) associated with each stream gauge. The TI and PI were calculated from gridded monthly temperature (°C) and precipitation (mm) absolute anomalies with gauge location determining the relevant grid cell. The TI was calculated as the average temperature anomaly in a gauge-specific four-month interval, which included the month of the respective CT at each stream gauge, as well as the two months prior and the month following the month of CT. The PI is the OA average precipitation anomaly for the

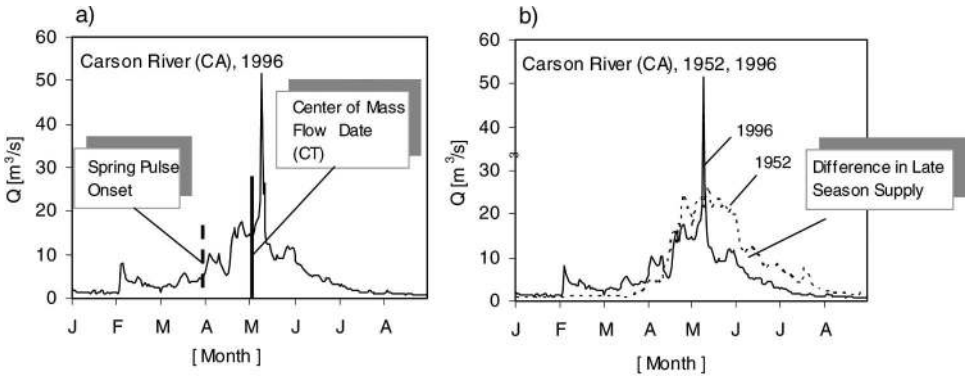

FIG. 1. Hydrographs of the (a) 1996 and (b) 1952 vs 1996 streamflow in the Carson River, West Fork, USGS gauge 10310000. In (a) the date of center of mass of annual flow (CT) and spring pulse onset timing measures of streamflow timing are indicated by the vertical solid and dashed lines, respectively.

grid cell. Other time intervals for TI and PI were tested, but correlations with CT were either comparable (in the case of PI) or less (TI).

To determine the influence of larger-scale climate, CT variations were also correlated with the ENSO (SOI) and Pacific decadal (PDO) modes as well as GSST. To assess the relative importance of the local and global influences, variations attributable to each of the climate indices TI, PI, PDO, SOI, and GSST were subtracted from CT, and that of PDO, SOI, and GSST from TI and PI, according to

$$Y' = Y - [\rho_{XY}(\sigma_Y/\sigma_X)]X. \quad (2)$$

Here Y is the variable from which the variations attributable to X are subtracted to yield the residual Y', where Y and X represent (CT, TI, or PI) and (TI, PI, PDO, SOI, or GSST), respectively: ρ_{XY} is the correlation coefficient between X and Y, and σ is the standard deviation. The residual CT time series were recorrelated with other climatic indices. All correlations were tested for statistical significance with two-tailed Student's t tests.

A PCA of the year-to-year variations of each of the three measures (fractional flows, spring pulse onset, and CT) were used to characterize their patterns of coherent variability. The empirical orthogonal functions (EOFs) found by each PCA were used to identify the most dominant and regionally extensive patterns of the year-to-year variability for each measure. The focus of this analysis is on the leading EOFs, which explain the largest portion of the variance. The principal component (PC) time series corresponding to each EOF was calculated as the standardized weighted sum of anomalies over the study area.

To examine the relationship between the regional variations of streamflow timing and large-scale climate anomalies, the leading PCs were used to construct composites (Livezey et al. 1997) of winter (DJF) and spring (MAM) temperature, precipitation, and 700-mb height anomalies. Atmospheric circulation patterns inferred from 700-mb heights have been linked to hydroclimatic signals (i.e., McCabe and Fountain 1995). Composites were generated by averaging the values of a given climate variable for the years with the 10 highest (lowest) values of leading PCs to provide a quantitative measure of large-scale, seasonal climatic anomalous conditions associated with extremes in the PC time series and were correlated with the time series of the corresponding PC. Correlations between the leading principal components of streamflow timing and the PDO, SOI, and GSST indices were also calculated.

Because a critical issue that emerges is the question of whether streamflow timing changes can be primarily attributed to fluctuations in the PDO, we compare the time histories in PDO and GSST (as a proxy for global warming trends) by evaluating the contributions that PDO makes to the CT trends and by comparing the average CTs during various PDO epochs. Particular attention is given to the recent shift of PDO in 1999 from its positive to its negative phase. Gauge-specific average CTs for periods having distinct PDO phases (1948–76, 1977–98, and 1999–2002) were calculated. The differences in average CTs for each gauge and PDO period served to establish the time-averaged response of CT to the decadal PDO fluctuations, as well as over the entire study period. Because simply fitting trend lines to PDO and CT or TI could overstate the role of PDO as a cause of the CT trends by inadvertently accommodating the 1976–77 PDO step change, we instead calculated the fraction of the observed TI and (separately) CT trends that are explained by the PDO step change trend, using coefficients from regressions of TI and CT with PDO during *subsets* of the 1948–2002 period during which PDO has little overall trend from

$$f_X = r_{X\text{-PDO}} \times (s_{\text{PDO}}/s_X), \quad (3)$$

where X stands for either TI or CT, f is the fraction of TI or CT trend explained by the PDO step change, $r_{X\text{-PDO}}$ is the correlation coefficient between TI or CT and PDO calculated separately for the 1948–76 and 1977–98 periods and then averaged, s_{PDO} is the slope of the trend in the PDO, and s_X is the slope of either the TI or CT time series. Neither the 1948–76 nor the 1977–2002 subsets of PDO trend positively or negatively, and thus TI–PDO (and CT–PDO) regression coefficients fitted to those periods provide measures of the year-to-year PDO influences.

4. Results

a. Trends in streamflow timing

Widespread trends toward both an earlier onset of the snowmelt spring pulse and earlier CTs are observed for snowmelt-dominated gauges (Fig. 2). The shifts are present throughout western North America for the 1948–2002 period. Trends toward delays in the spring pulse onset dates and CT are neither as large, as numerous, nor as widespread as those toward earlier dates.

The most prevalent trends in the spring pulse onset dates comprise a 10–30-day shift toward occurring earlier in the water year over the 55-yr study period (Fig. 2a). These trends are large throughout the western United States but largest in the Pacific Northwest and the Sierra Nevada. Shifts toward earlier spring pulse onset dates of more than 3 days are detected at 66% of the 241 gauges, while shifts toward later dates or no trends were indicated at 15% and 19% of the gauges, respectively. Due to the considerable interannual variability in the beginning of the spring pulse onset, illustrated in the examples of Figs. 3a–d, not all trends are significant at the 90% significance level, although the observed trends are large and show remarkable regional coherence. Of the 96 significant trends, 86 are negative. Trends toward later snowmelt pulse dates (5–

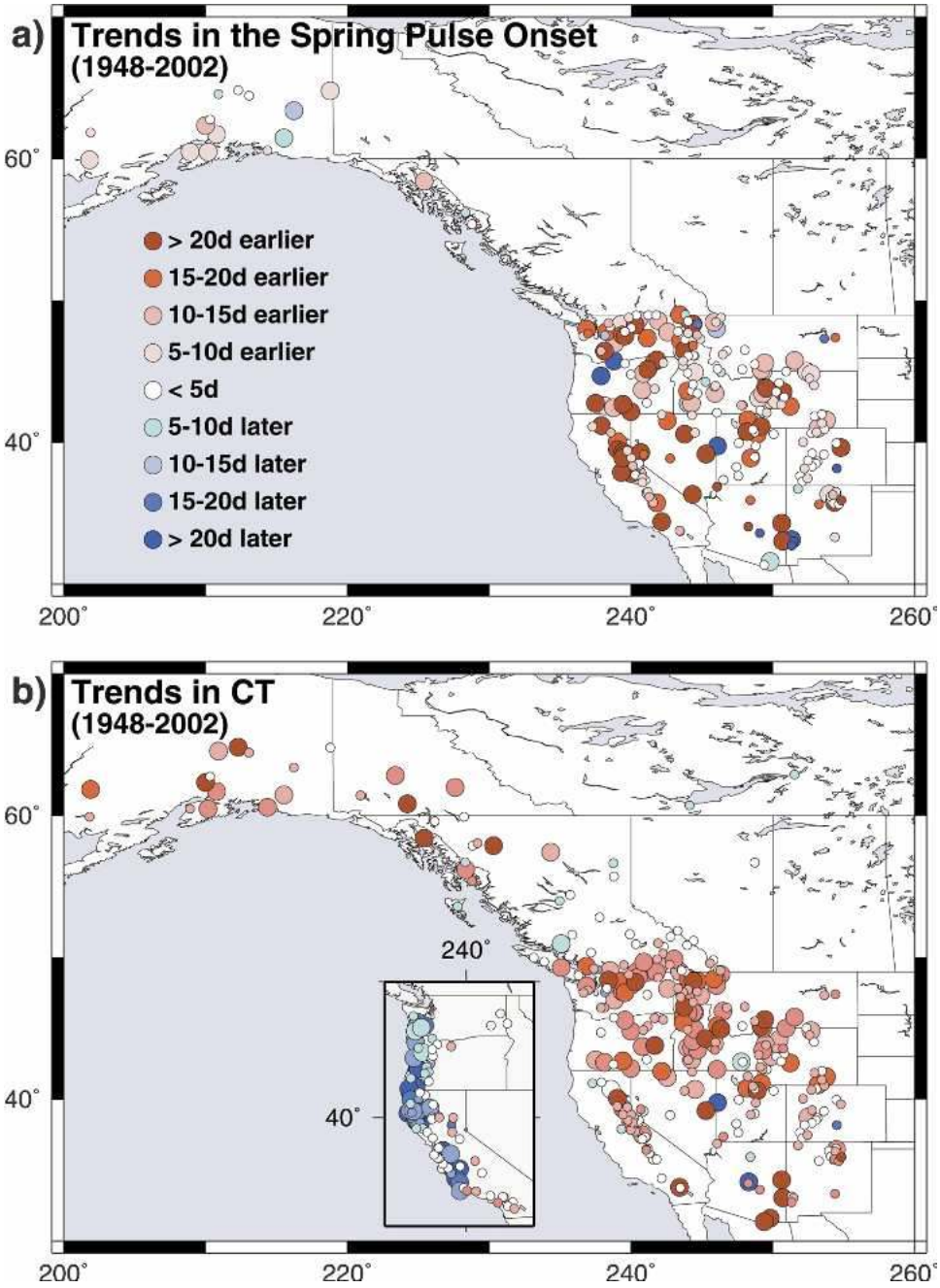

FIG. 2. Trends in (a) spring pulse onset and (b) date of center of mass of annual flow (CT) for snowmelt- and (inset) non-snowmelt-dominated gauges. Shading indicates magnitude of the trend expressed as the change (days) in timing over the 1948–2000 period. Larger symbols indicate statistically significant trends at the 90% confidence level. Note that spring pulse onset dates could not be calculated for Canadian gauges.

20 days over 55 years) are present for isolated gauges in the Southwest, Oregon, and Alaska.

Trends in CT for snowmelt-dominated basins (Fig. 2b, main panel) correspond well to trends in the snowmelt pulse dates and in average fractional flows with respect to their spatial distribution, magnitude, and direction. The densest clusters of large trends, corresponding to shifts of 10–30 days, were observed for rivers in the Sierra Nevada, the Pacific Northwest, and coastal Canada and Alaska. Trends toward earlier CT dates with shifts of more than 3 days are detected at 73% (214) of the gauges (105 are significant), while

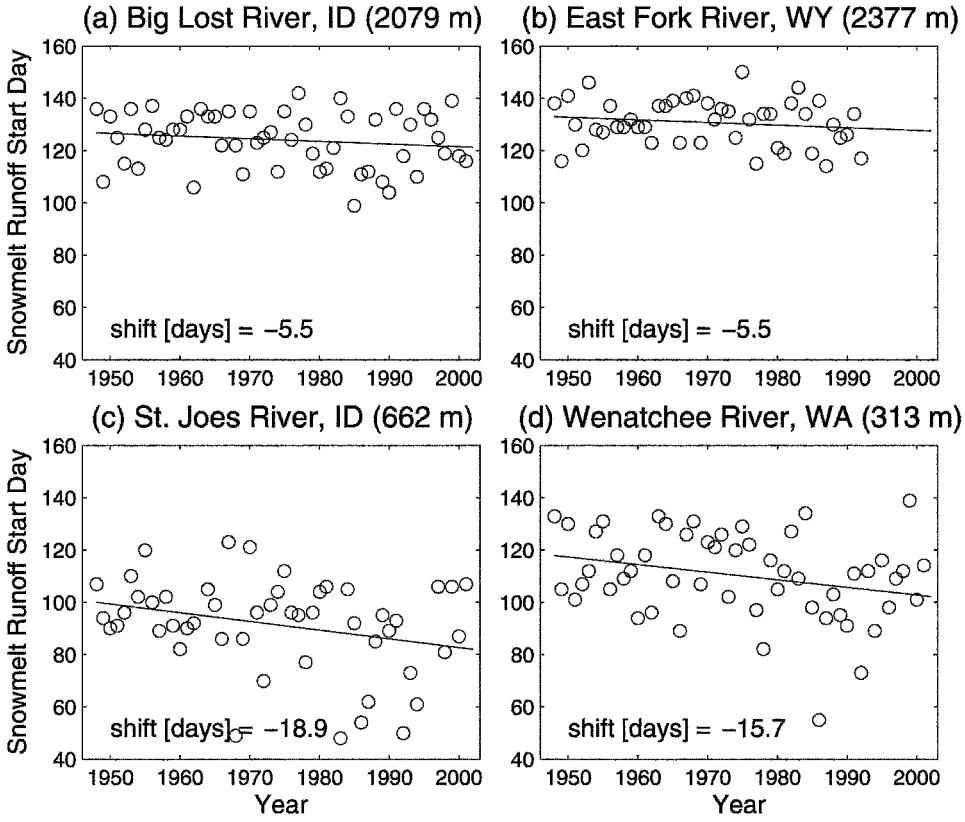

FIG. 3. Observed spring pulse onset dates for (a), (b) two high- and (c), (d) two midaltitude stream gauges, illustrating differences in magnitude of the observed time shift.

advances of less than 3 days occur at 18% of the gauges. Shifts toward later dates occur at only 9% (26) of the gauges. Few trends toward later CTs were found for isolated gauges in the Sierra Nevada, the New Mexico–Colorado region, and Canada. By contrast, for non-snowmelt-dominated streams, CTs at most gauges (Fig. 2b, inset) are trending in the opposite direction, toward later snowmelt timing, with shifts to 5–25 days later. Available data for the 1901–2002 period (not shown) reveal overall trends toward earlier streamflow timing for the coastal states and smaller or no trends for gauges in the interior. The amplitude of the timing changes increases after the mid-1940s.

To illustrate how streamflow timing changes vary with basin location and elevation, Fig. 3 shows the 1948–2002 spring pulse onset dates for two high-altitude (Big Lost River, Idaho, and East Fork River, Wyoming) and two midaltitude (St. Joe River, Idaho, and Wenatchee River, Washington) basins. The high-elevation basins have later mean onset dates since they remain well below freezing throughout the spring and thus are less affected by temperature changes early in the season. Correspondingly, the shift in start day for the Big Lost and East Fork Rivers is relatively small, only 6 days earlier. By contrast, lower altitude basins such as the St. Joe and Wenatchee River basins have earlier mean onset dates and are more sensitive to small temperature changes. The snowmelt pulse at the St. Joe and Wenatchee River basins advances by 19 and 16 days, respectively, by the end of the study period. The relationship between basin elevation and the magnitude of its trends exists between nearby streams, such as the Big Lost and St. Joe Rivers, which presumably are influenced by the same regional climatic regimes, but also exists for basins that are far apart and that are under the influence of very different regional climatic regimes (see also Fig. 2), such as the East Fork and the Wenatchee Rivers.

Consideration of the average seasonal (AMJJ) March and June fractional flows and their trends (Fig. 4) yields more insight into the hydroclimatic shifts. The average flow fractions shown in the upper panels of Fig. 4 illustrate that for most snowmelt-driven watersheds in western North America, AMJJ flows are the most important contribution to the annual streamflow, comprising 50%–80% of the annual total (Fig. 4a). In contrast, at non-snowmelt-dominated gauges, mean AMJJ flow fractions are less than 30%, except in Alaska. The AMJJ fraction is not as suitable a measure of the snowmelt discharge component for gauges located north of 50°N latitude, where, on average, snowmelt-derived streamflow does not commence until May and contin-

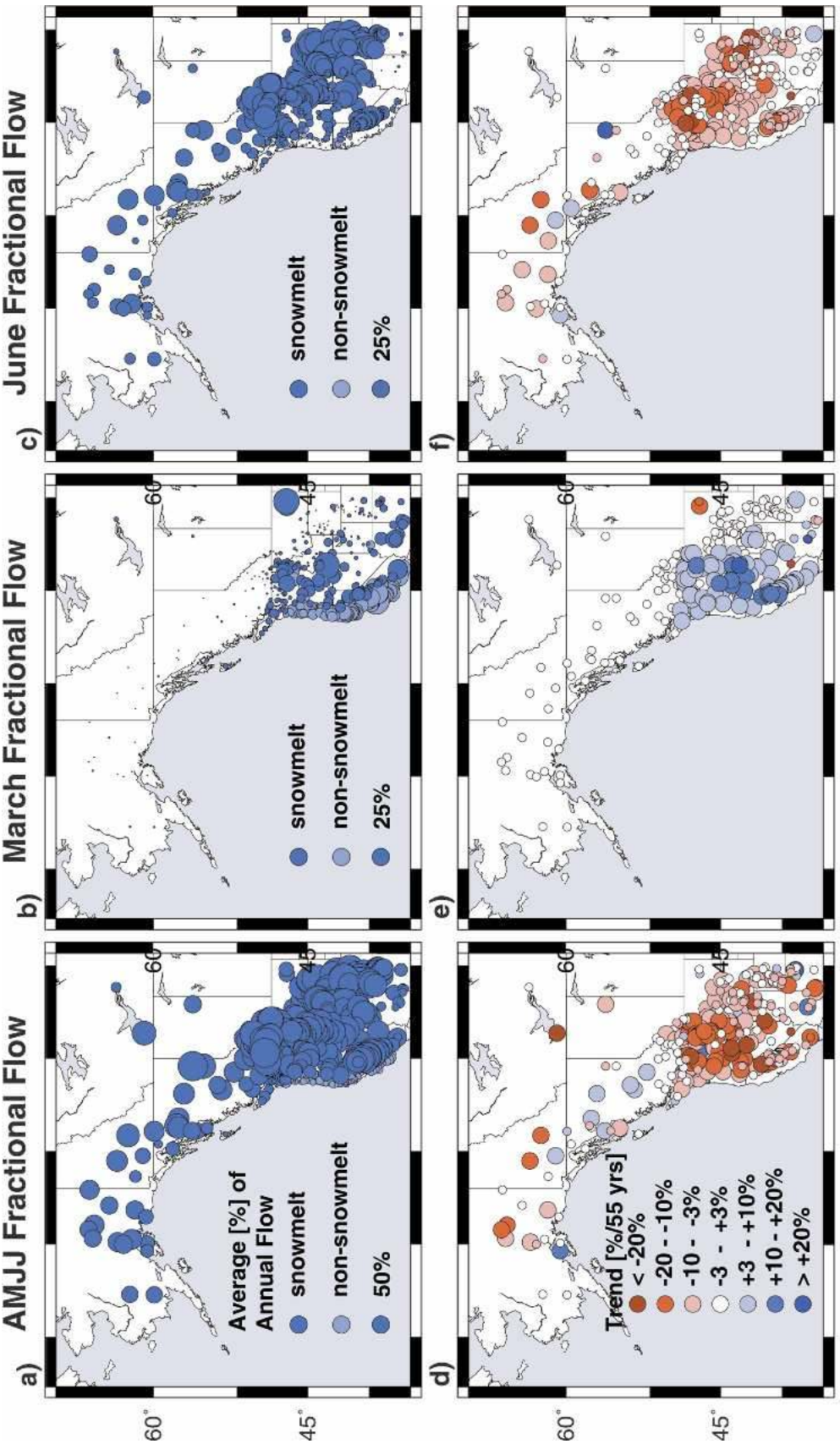

FIG. 4. (top) Mean seasonal and monthly flow fraction of total annual discharge for (a) AMJJ, (b) Mar, and (c) Jun. (bottom) Trends in the seasonal and monthly flow fractions for (d) AMJJ, (e) Mar, and (f) Jun.

ues through August or September. Many of the AMJJ fractional flow trends (Fig. 4d) are statistically significant at the 90% level. The largest trends toward decreasing AMJJ fractional flows are found in the Sierra Nevada, eastern Oregon, and the central Rocky Mountains. The observed slight increase of AMJJ fractional flow for some high-latitude Canadian and Alaskan gauges is partly caused by a shift within the primary northern May through August snowmelt season to earlier in the water year (especially May). This shift is similar to that at the lower latitudes but is delayed until later in the water year. An important accompanying piece of evidence is that for the nonsnowmelt streams, trends have been generally small, with only a few significant changes in either seasonal or monthly flow fractions. Although 81% of the snowmelt-dominated gauges exhibit negative trends for the AMJJ fractional flows, annual (water year) flows have generally shown increasing trends, except for the Pacific Northwest portion of the domain. About 50% of the stream gauges with decreasing AMJJ fractional flow trends show slight to moderate trends toward increasing annual total flow.

The most extensive, regionally coherent increases in monthly fractional flow occur in March (Fig. 4e). This widespread sensitivity and coherence of March flow fractions occurs even though March fractional flow is comparatively small (<10%) for most snowmelt-dominated streams south of about 50°N latitude and is even less for gauges farther north, where March precipitation is probably stored as snowpack (Fig. 4b). A corresponding increase in monthly fractional flow for the northern and higher-elevation rivers, where cooler temperatures delay the average snowmelt season by 1–2 months, is found in May (not shown). Average May fractional flows at the high-elevation and northern gauges reach 10%–30% and contribute strongly to both snowmelt-derived streamflow and annual flow. Thus, for many northern and high-elevation gauges, the trends toward increasing May fractional flows reflect the shifts toward earlier snowmelt. Average June fractional flow represents a significant portion, 10%–30% for many gauges, of average annual flow for the snowmelt-dominated gauges, as shown in Fig. 4c. The sizable and widespread trends toward decreasing June fractional flows appear to be a compensation for the increase in fractional flow during March through May as snowmelt basins begin to run out of water, and therefore reflect substantial changes in the temporal distribution of flow. Decreases in June average fractional flow range from 5% to 25%, as shown in Fig. 4f.

b. Responses of streamflow timing to local climate anomalies

The timing of snowmelt is likely affected both by precipitation and temperature (i.e., Hamlet and Lettenmaier 1999) but, since they may be correlated, it is not immediately clear which of these two influences dominates the observed CT variations. While temperature increases advance the timing of snowmelt, increased winter precipitation falling as snow results in an increased snowpack and generally a delay in the spring runoff. To characterize seasonal temperature and annual precipitation influences, TI and PI were analyzed and correlated with CTs at each gauge. Both TI and PI display trends over most of the study region (not shown). The TI trends are increasing throughout the domain, corresponding to a warming of 0.5°–2.0°C over the 55-yr period. Relative to its variance, PI trends are smaller than those for TI [$\pm$0–8 cm (55 yr)$^{-1}$]. Significant positive trends are found in the south of the study area and Alaska; significant negative trends in the Pacific Northwest and western Canada. The TI and PI indices are inversely correlated (-0.2 to -0.6) for many Rocky Mountain gauges in the domain, as shown in Fig. 5a, such that higher seasonal temperatures around the timing of the center of mass are associated with anomalously low winter precipitation. Mild positive correlations between TI and PI occur in south-central Alaska where warmer, and therefore moister, air masses combine to bring precipitation to these northern coasts. The relationship between CT and PI is complex and regionally dependent. As shown in Fig. 5b, CT and PI are positively correlated (0.2–0.8) in rivers throughout the Sierra Nevada and Rocky Mountains, but it is noteworthy that no substantial precipitation trends were found in these areas. Negative correlations between CT and PI were found for the Canadian, Alaskan, and Pacific Northwest coastal areas and the Arizona region. Positive correlations indicate that snowmelt and snowmelt-fed streamflow tend to occur later with increasing winter precipitation.

The most remarkable connection between streamflow timing changes and local climate forcings was found to involve spring temperature anomalies before and during the spring melt period. Strong and regionally coherent correlations between the individual time series of CT and TI are present (Fig. 6a) throughout the domain, with the generally highest correlations for gauges south of 52°N. The correlations range from -0.3 to -0.8, in the sense that higher temperatures (higher TI) are associated with earlier streamflow timing (CT). In contrast to changes associated with temperature anomalies, CT shifts associated with observed precipitation variations over the region are mostly in the opposite direction, as illustrated by the trends toward later CT for the nonsnowmelt-dominated gauges in the study area (Fig. 2b, inset). Thus, streamflow timing would tend to be later if it were only influenced by the timing of precipitation. Notably, the magnitude of the temperature change working on snowmelt-dominated basins is strong enough to overwhelm the precipitation effect. The strong correlations between CT and TI remain essentially unchanged when the portion of the variance that is linearly related to PI is removed (Fig.

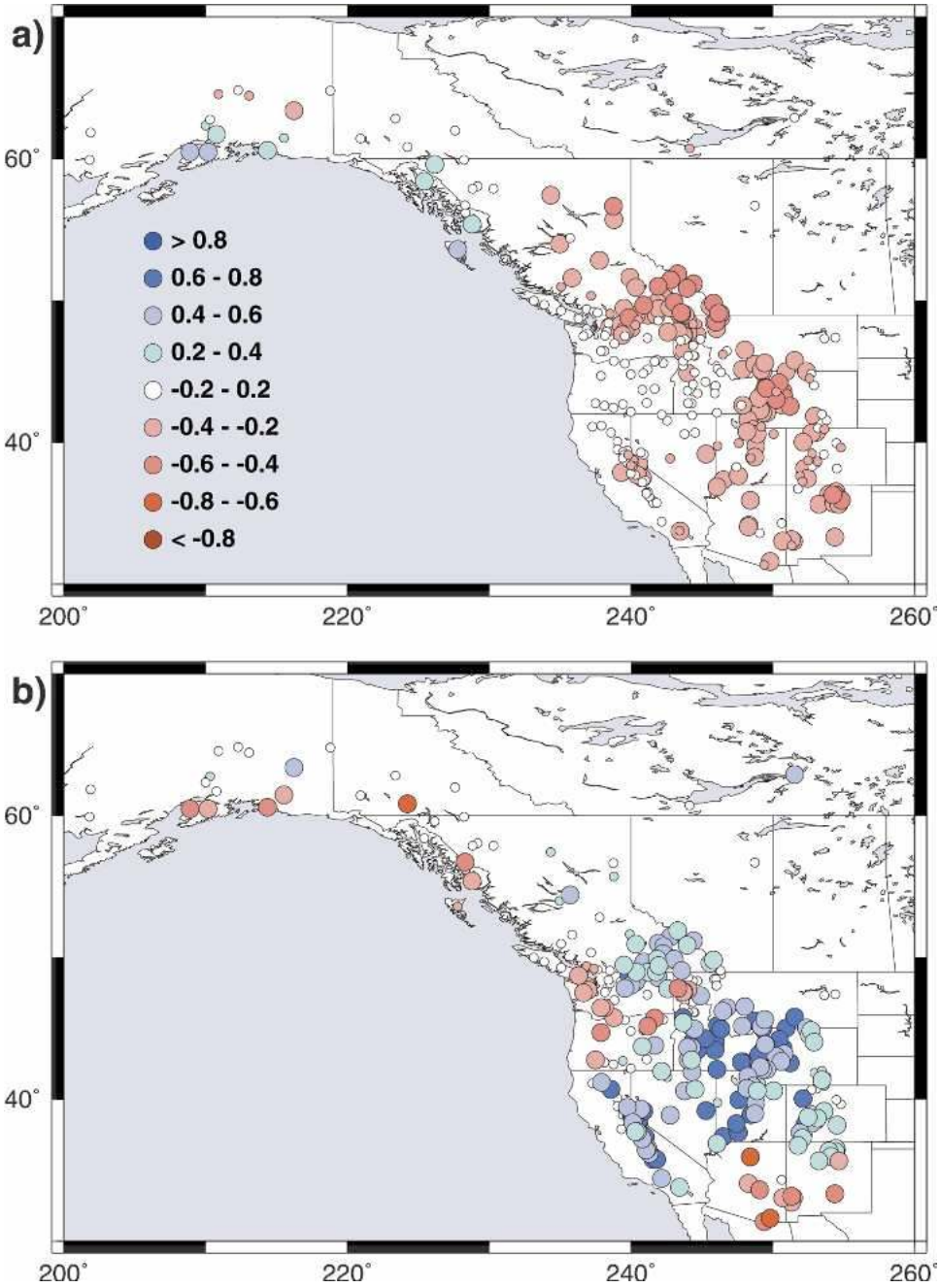

FIG. 5. Correlations of (a) temperature indices (TIs) with precipitation indices (PIs) and (b) CT with PI. Larger symbols indicate statistically significant correlations at the 95% confidence level.

6b). On the other hand, correlations between CT and PI are decreased by 5%–10% for most gauges if the variation of CT related to TI is first subtracted (not shown). Smaller reductions were found for most gauges located in the northernmost latitudes, which are colder and hence less susceptible to moderate temperature and precipitation changes.

A different measure of local conditions relating to snowmelt timing is provided by the measured snow water content at or near the onset of snowmelt. The correlations in Fig. 7 show that greater winter snow-water equivalent (SWE) is quite strongly associated with later snowmelt and CT timing date for most gauges in the Sierra Nevada, Rocky Mountains, and Canada, even very early in the snowmelt season (1 February). A similar but even stronger linkage exists for snow accumulations later in the spring (i.e., 1 April SWE; not shown). For northern Canada and Alaska, a less-than-

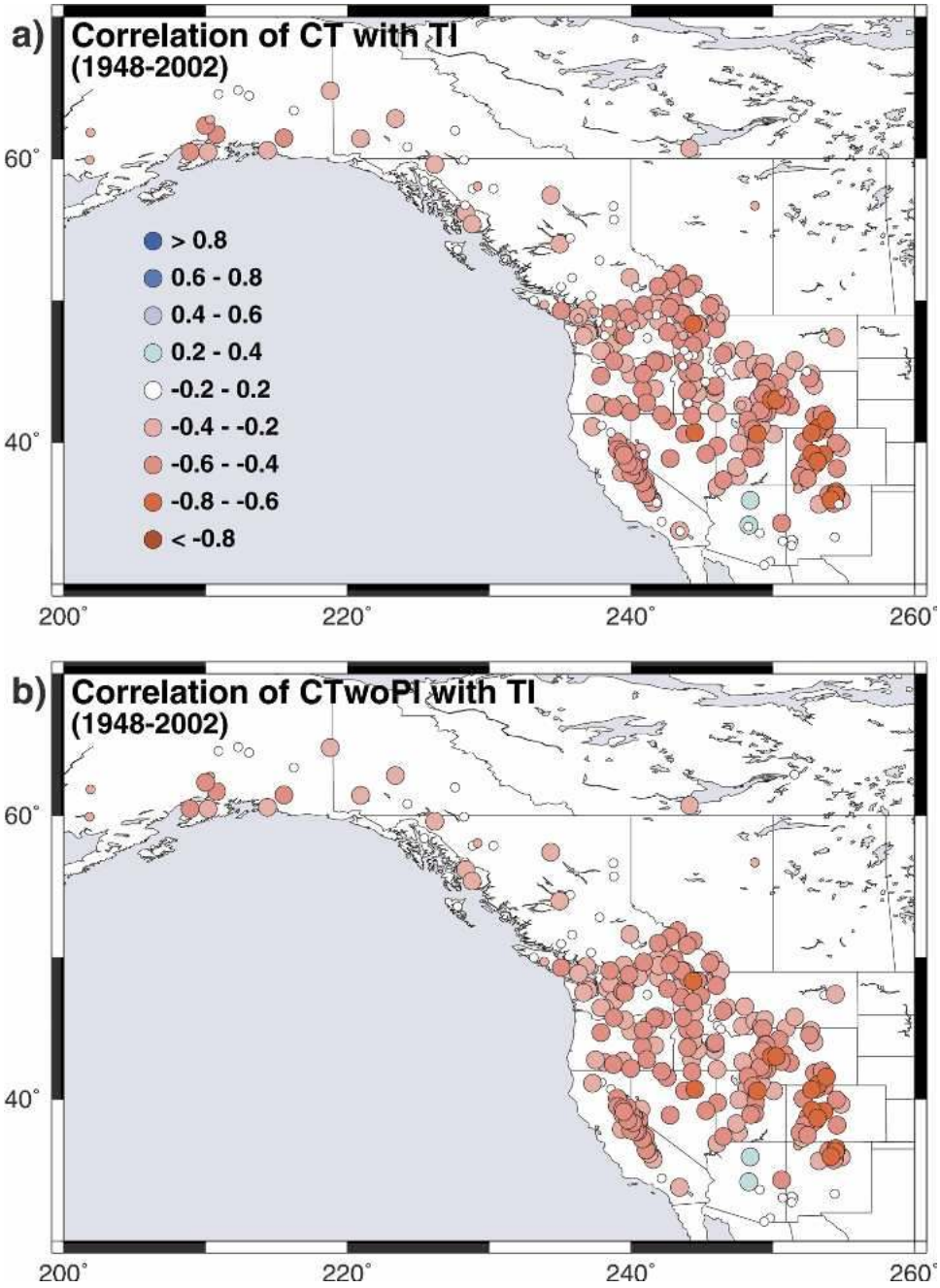

FIG. 6. Correlation of (a) CT with TI and (b) CT minus the portion of its variance attributable to the PI (CTwoPI), with TI. Larger symbols indicate statistically significant correlations at the 95% confidence level.

average snowpack is associated with later streamflow timing, presumably due to the association of very cold with dry conditions there.

c. Connections to Pacific basin climate

Much of the interannual and lower-frequency climate variability over western North America is driven by Pacific climate patterns. Considering the correlations between the CT with TI and PI, it is not surprising that CT also exhibits significant correlations with the SOI and PDO indices. Both SOI and PDO are associated with distinct temperature and precipitation patterns throughout western North America (Ropelewski and Halpert 1986; Redmond and Koch 1991; Latif and Barnett 1994; Mantua et al. 1997; Cayan et al. 1999). The positive phase of the PDO is associated with higher

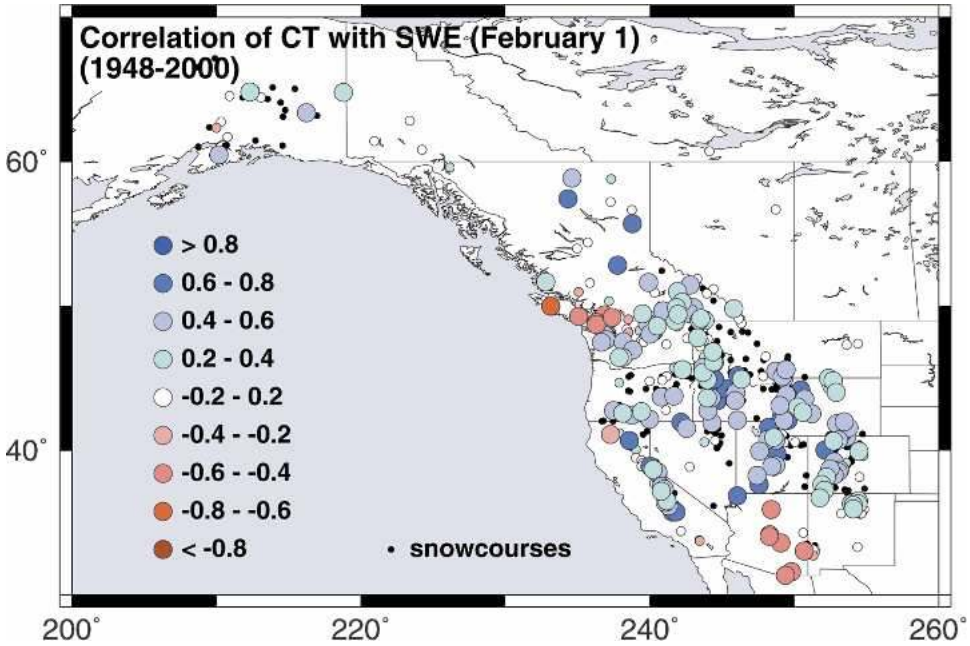

FIG. 7. Correlations of CT with 1 Feb snow-water equivalent (SWE) at the nearest snow course. Small black symbols are locations of snow courses. Larger symbols indicate statistically significant correlations at the 95% confidence level.

temperatures over the western North American continent (Mantua et al. 1997) and cooler temperatures over the Southwest. Thus PDO and CT tend to be inversely related ($r = -0.2$ to -0.8; see Fig. 8a). This relationship is strong and statistically significant for many gauges in the study domain except for those in the Southwest. The north–south seesaw precipitation contrasts associated with theENSO (Redmond and Koch 1991; Dettinger et al. 1998) is reflected in the spatial pattern of CT correlations with the SOI, shown in Fig. 8b. Negative SOI, or El Niño, conditions are associated with warmer spring temperatures and lower winter precipitation in the northern portion of the study area and therefore with earlier snowmelt-derived streamflow, leading to positive correlations with CT ranging from $r = 0.2$ to $r = 0.6$. In the southern portion of the study area, negative SOI conditions are associated with higher-than-average winter precipitation, leading to a delay in snowmelt and negative correlations with CT ranging from $r = -0.2$ to $r = 0.6$.

d. Regionally coherent streamflow timing variations

Interannual and longer period variations in snowmelt timing tend to vary coherently among many streams over a large region in western North America. A separate PCA of CT, spring pulse onset, and fractional flows illustrate this extensive spatial coherence with just a few spatial patterns needed to explain a substantial portion of the total variance. Large fractions of the variability of all four streamflow timing measures are shared, large-scale variations. Figure 9a, EOF1 of CT, shows broad regions of shared variability, with largest weights over the central and northern Rocky Mountains and the Sierra Nevada. This first EOF explains 26%, and the first four EOFs explain over 50% of the total variance. Correlations of the first four PCs of CT against PDO, SOI, GSST, and the first principal component of TI are summarized in Table 1. The large-scale shared variability captured by the significantly trending PC1 (Fig. 9b) is somewhat anticorrelated with the PDO ($r = -0.25$) but is more anticorrelated with the large-scale common variability in spring temperature described by PC1 of TI ($r = -0.38$). The significantly trending PC2 may be related to both SOI and GSST ($r = -0.37$ and $r = 0.30$, respectively), while PC3 is also modestly correlated with both SOI and GSST ($r = 0.32$ and $r = 0.20$, respectively).

A composite analysis of 700-mb height anomalies reveals that CT is statistically significantly correlated with specific winter and spring atmospheric circulation patterns (Fig. 10). Temperature composites (not shown) are consistent with the circulation composites. Low PC1 values (widespread occurrence of earlier CTs) are associated with positive 700-mb height anomalies across western North America (Fig. 10a), which result in warmer winter and spring temperatures and earlier snowmelt and streamflow. High PC1 values, corresponding to later CTs, are associated with positive 700-mb height anomalies over the North Pacific and with negative 700-mb height anomalies over western North America, which reflects the presence of colder air

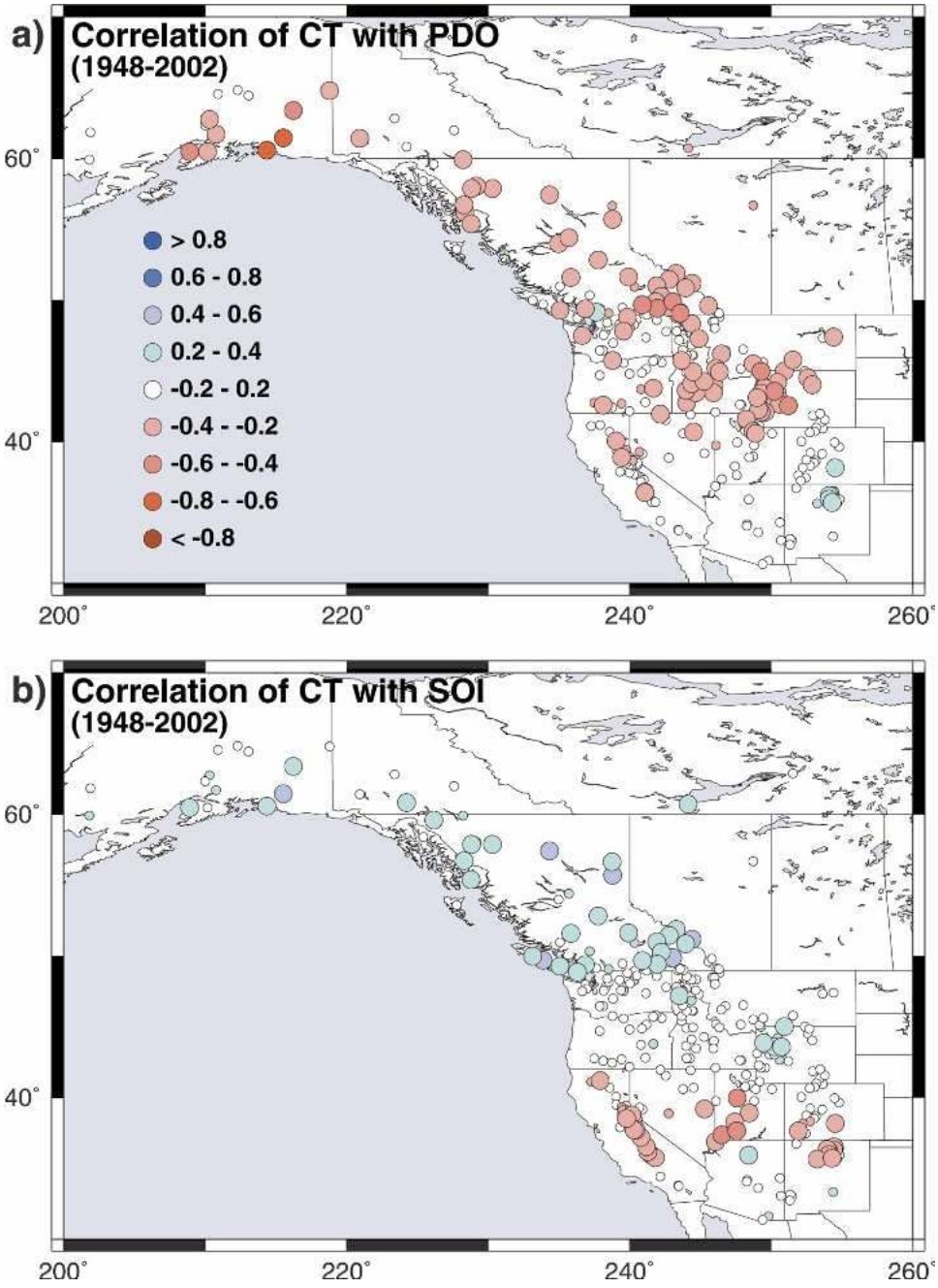

FIG. 8. Correlations (−) of (a) CT with average water year PDO index and (b) CT with average Oct–Mar SOI. Larger symbols indicate statistically significant correlations at the 95% confidence level.

masses and generally wetter conditions over the study region.

e. PDO versus global climate influences

The strong correlations of CT to both springtime temperature (TI) changes and decadal-scale fluctuations (PDO) raise the question whether the observed changes in CT are driven primarily by PDO-related temperature changes or by some other mechanism. Our analysis suggests that PDO contributes to some of the observed CT trends but is not sufficient to explain them all. To clarify this issue, various analyses are conducted to compare the associations of CT and PDO with those of CT and temperature (through TI and GSST).

During the 1951–2000 period emphasized here (as well as in the earlier 1901–40 period), GSST and PDO are correlated ($r = 0.5$), and over the 1948–2000 period, both trend markedly. The GSST and PDO are not cor-

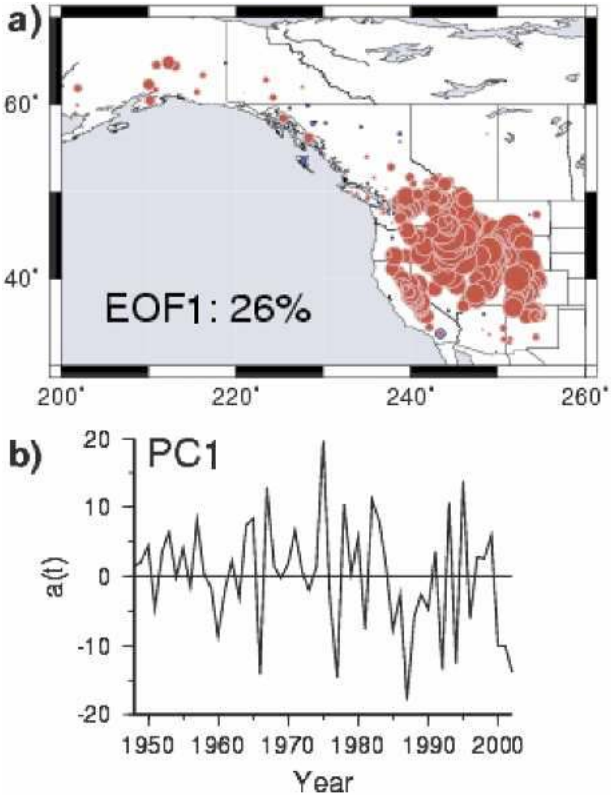

FIG. 9. (a) Spatial loading EOF1 from principal component analysis (PCA) of CT. The percent of CT variance explained by the first PC is listed. Red and blue symbols refer to positive and negative loadings, respectively. (b) The time series of PC1.

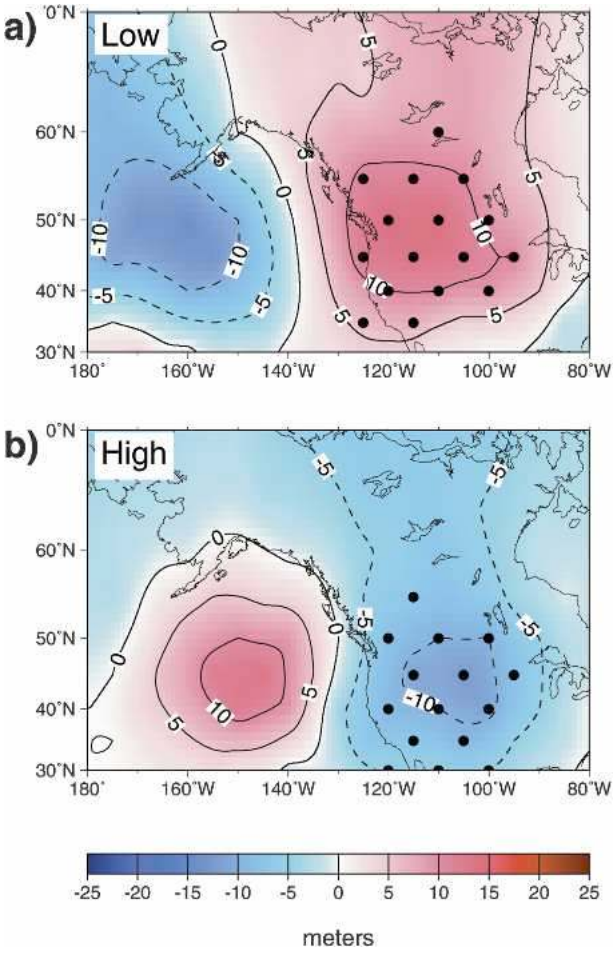

FIG. 10. Composites of spring 700-mb height anomalies for (a) low and (b) high values of PC1 associated with (a) earlier and (b) later timing of snowmelt-derived streamflow. Statistically significant correlations at the 95% confidence level are marked with small black circles.

related over the entire 1901–2000 period, but this is largely due to a marked jump (possibly spurious) in the 1940s GSSTs, coincident with (and opposite to) a PDO transition to its cooler phase. The PDO "trend" over the 1951–2000 period is for the most part the result of the well-known cool-to-warm 1976–77 PDO step change (Mantua et al. 1997) that yields a net positive trend when judged by linear regressions. Subtracting the CT variations associated with either PDO or GSST from CT [Eq. (2)] leaves no significant (residual) CT trends. Overall, correlations of CT with GSST ($r = -0.2$ to $r = -0.6$) are weaker than those of CT with PDO ($r = -0.2$ to $r = -0.8$), which are weaker than those of CT with TI ($r = -0.2$ to $r = -0.8$) in terms of both the number of gauges with significant correlations and the strength of the correlations at a given gauge. Subtracting the GSST component from each of the CTs reduces the magnitude of the CT–PDO correlations by 5%–50% (not shown). Removing the variance attributable to GSST from TI results in weaker correlations (5%–60%) to the PDO index than the original TI. These findings could be an indication that PDO and GSST are not entirely independent and that effects of PDO on streamflow timing cannot be completely separated from a warming trend. However, all three series include significant trends over the 50-yr period, and since any two trends are correlated, attribution of the causes of CT trends requires closer attention.

The relative contributions of the PDO and other TI variations on CT variability are suggested by subtracting the CT variance attributable to TI from CT [Eq. (2)] and correlating the residual with the PDO. Removing the overall TI influence in this way almost entirely re-

TABLE 1. Correlation of leading streamflow timing (CT) PCs with the PDO, SOI, GSST, and the first principal component of the TI. Significant trends and correlations at the 95% confidence level given in boldface.

PC	Trend ($\times 10^{-2}$)	PDO	SOI	GSST	PC1 of TI
1	**−1.4**	**−0.25**	0.01	**−0.23**	**−0.38**
2	**1.2**	0.17	**−0.37**	**0.32**	0.17
3	−0.1	0.10	**−0.30**	0.22	−0.01
4	−0.3	**−0.33**	**−0.26**	−0.07	0.18

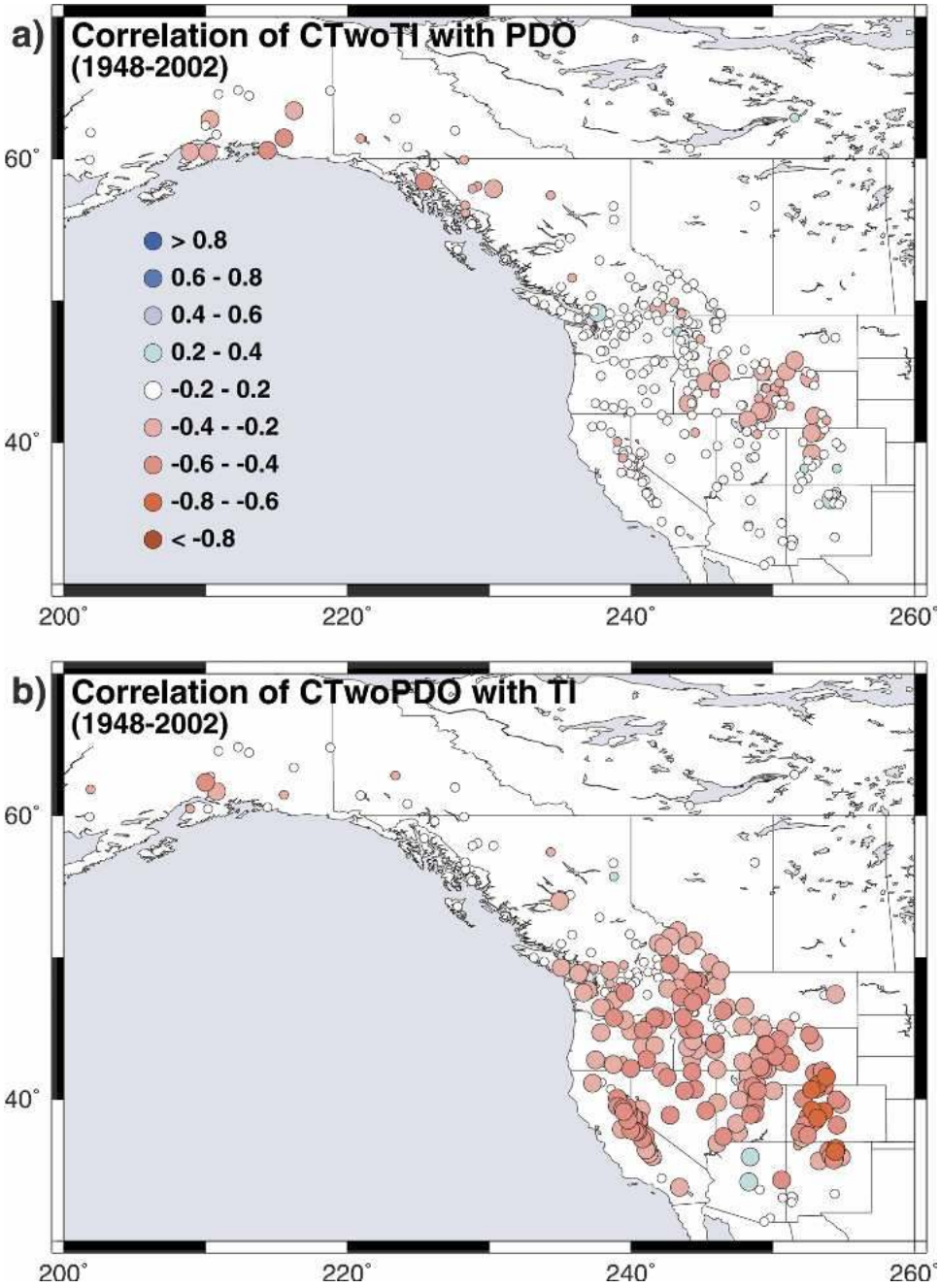

FIG. 11. Correlation of (a) CT minus the portion of its variance attributable to the TI (CTwoTI), with PDO and (b) CT minus the portion of its variance attributable to the PDO index (CTwoPDO), with TI. The larger symbols indicate statistically significant correlations at the 95% confidence level.

moves the CT–PDO connection, except for some Canadian and Alaskan gauges (cf. Fig. 11a and Fig. 6a). Thus, nearly all PDO influence on CT is temperature driven. Interestingly, though, if the CT variance that is attributable to the PDO is first removed from CT and that new CT is correlated with TI, the CT–TI correlations are reduced only modestly (Fig. 11b). These results suggest that observed CT variations are responses to changes in TI that, at least in part, are not driven by the PDO.

Examining the fraction of the TI and CT trends explained by the PDO step change [Eq. (3)], less than half of the observed TI trends are attributable to PDO for most gauges (Fig. 12a) except in the northwestern U.S. area where PDO is known to have the greatest influence (e.g., Mantua et al. 1997; McCabe and Dettinger

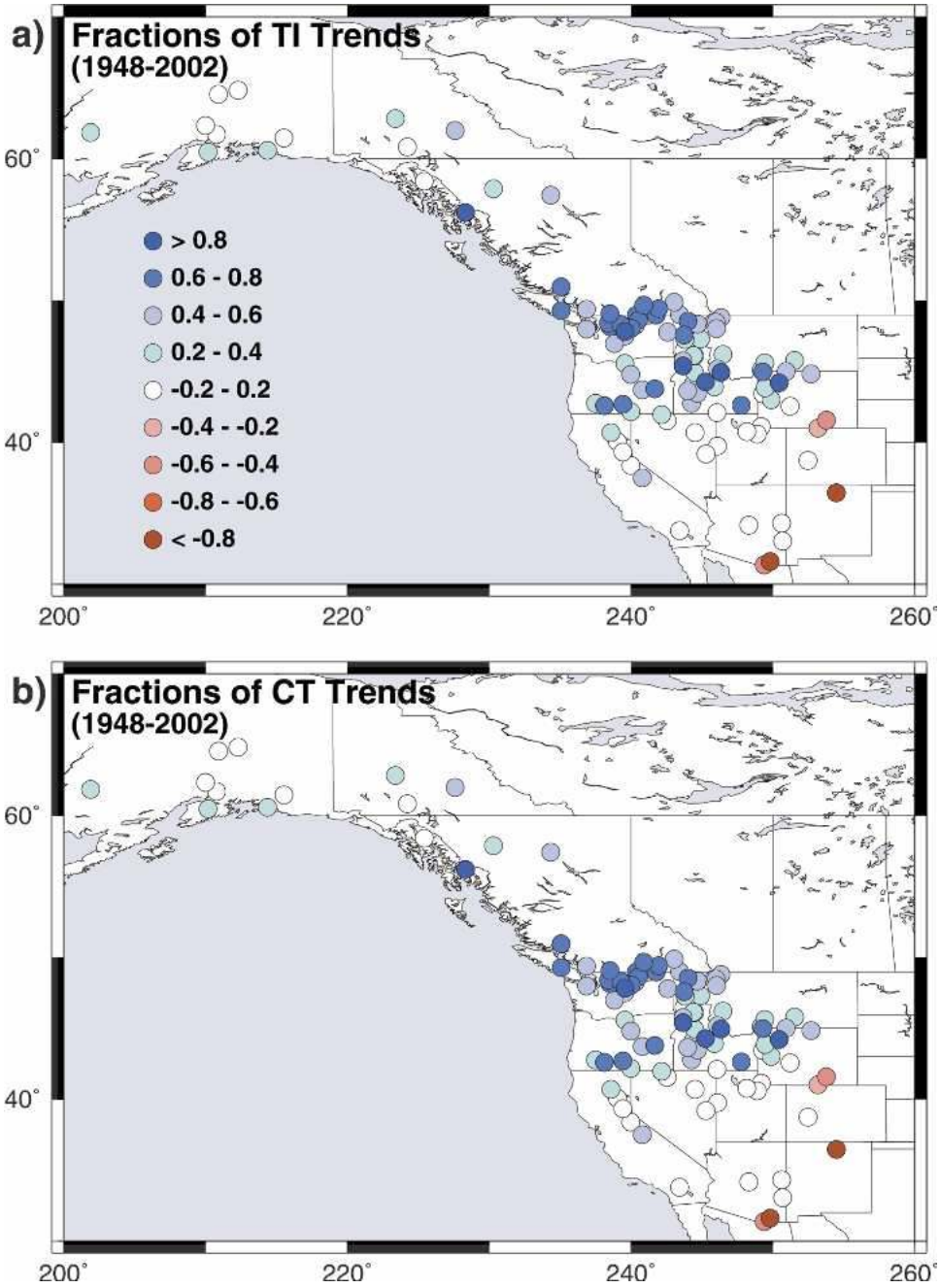

FIG. 12. Fractions of observed (a) TI and (b) CT trends that are explained by the PDO step change trend, using coefficients from regressions of CT and TI with PDO. Regression coefficients averaged from those calculated for 1948–76 and the 1977–98 periods. Fractions are shown only for gauges with significant observed CT trends.

2002; Mote 2003b). Similarly, less than half of most significant trends in CT throughout the study area can be attributed to the PDO with the exception of some gauges in south-central Alaska and the northern Rocky Mountains (Fig. 12b). "Negative fractions" can be calculated if the sign of the regression coefficient for one (or both) of the 1948–76 or 1977–2002 subperiods is opposite that of s_X, indicating no influence of the PDO on the TI or CT trend.

The influence of PDO on the CT trends can also be examined by considering the effect of a recent shift of PDO from positive to negative phases in 1999 and the disposition of CT in association with the individual PDO modes in the study period. In contrast to the

PDO, neither greenhouse gas forcings nor global temperatures (or GSST) have reversed since 1999. Thus, if CT timing changes were dominantly controlled by the PDO and the advances of the average CT were mainly a response of the cool-to-warm 1976–77 PDO switch, then streamflow timing would be expected to also revert—toward later CTs again—during the cool 1999–2002 PDO phase. Following the 1999 PDO reversal, the CTs for each of the 2000–02 water years continued to be early or very early, except for a small area in the Pacific Northwest (not shown), an area that is quite strongly affected by the PDO. In addition, over the 1977–2002 period since the Pacific climate shift, TI has trended toward warmer and CT has trended toward earlier for most western streams (not shown). Scatterplots of CT anomalies and TI from 1948 through 2002 (Figs. 13a, b) illustrate that the trends in CTs and TIs continued through 2002. The exception is a region centered on the Pacific Northwest and southwestern Canada, where CTs during 1999–2002 have later snowmelt runoff. Considering the whole study period, temporally averaged CTs in the warm (1977–98) PDO period were earlier than those in the earlier (1948–76) cool period for almost all gauges in the study (Fig. 13c), but average CTs throughout most of the study area came even earlier during the recent (1999–2002) cool PDO period than in the preceding warm PDO epoch (Fig. 13d). Thus, the recent PDO reversal has not reversed the observed streamflow timing anomalies. This suggests that PDO shifts are not the only source of the CT (and TI) trends.

5. Conclusions

By several different measures, long-term shifts in the timing of streamflow have been observed for snowmelt-dominated basins throughout western North America since the late 1940s [see also the recent studies by Mote (2003a) and Regonda et al. (2005)]. These shifts represent an advance to earlier streamflow timing by one to four weeks in recent decades relative to conditions that prevailed in the 1950s through the mid-1970s. Earlier flows are observed throughout the mountainous parts of the region, but trends are strongest for midelevation gauges in the interior Northwest, western Canada, and coastal Alaska. Streamflow timing has shifted toward occurring earlier in the water year at most snowmelt-dominated gauges across an area much larger than previously recognized, while mean annual flows have remained constant or marginally increased. Evidence for the shift includes earlier snowmelt onsets and advances in the center of mass of the annual hydrograph, which is called center timing (CT). Consistent with these advances are decreased spring and early summer (AMJJ) fractional flows and increasing fractions of annual flow occurring earlier in the water year. The months with the largest positive fractional flow trends in the western contiguous United States are March and April, while those in Canada and Alaska are April and May.

Importantly, streamflow timing records include considerable interannual variability in addition to a low-frequency change. These year-to-year streamflow timing variations are remarkably coherent across western North America, especially among southern Canadian, Rocky Mountain, Pacific Northwest, and Sierra Nevada rivers. These shorter-period variations in timing are controlled by regional precipitation anomalies and, to a much greater extent, by regional temperature fluctuations. Because these shorter-period interannual variations are presumably controlled by the same physical influences as the longer period changes, they provide an opportunity for calibrating the responses of streamflow timing to variations of temperature and other variables. From such calibrations, it has become clear that the primary cause for the regionally coherent trends toward earlier snowmelt and streamflow timing is a broad-scale increase of winter and spring temperatures by about 1°–3°C over the past 50 years. As shown herein and in a companion study (Stewart et al. 2004), this degree of warming is sufficient to advance the timing of CT in western North America watersheds by one to four weeks. Interestingly, changes due to temperature increases have overwhelmed opposing precipitation-driven changes over much of the western United States during the study period. Also associated with the warming and, thus, the earlier spring streamflow timing have been large regional changes in atmospheric circulation that have produced trends toward higher-than-normal pressure anomalies over western North America. A significant part of the long-term regional change in streamflow timing can be attributed to decadal climatic variations in the Pacific basin through the Pacific Decadal Oscillation (PDO), which have yielded decadal-scale changes in temperature. Yet, there remains a sizable residual fraction—in addition to natural variation—of the streamflow timing trend that is not explained by PDO and appears to be related to temperature increases consistent with observed changes in global temperature. Notably, the PDO was not found to be independent from a global warming trend represented by GSST over the past few decades. Attribution of the changes to either the PDO or a separate warming trend is impeded by the relatively long time scales of natural interdecadal variability in comparison to the five-decade study period, but the following evidence leads us to conclude that a large part of the western streamflow timing trends are not due to PDO:

1) In most western rivers, PDO accounts for a significant fraction of the variance in streamflow timing over a range of time scales from interannual to decadal, but not as much as local spring temperature (TI) variations do. Removing CT variations that are linearly associated with spring temperature fluctuations, and with the PDO, and then correlating TI

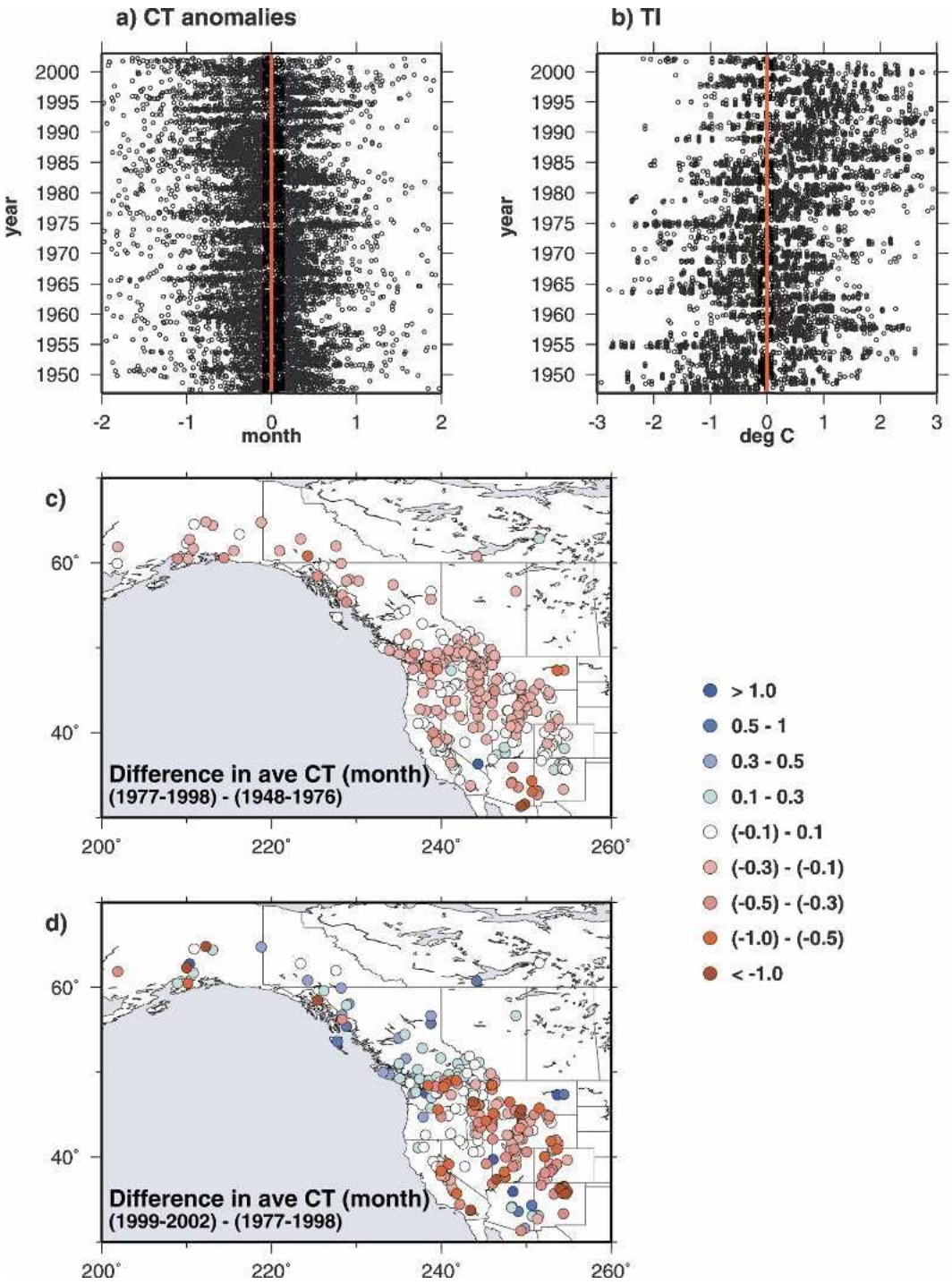

FIG. 13. (top) Time series of (a) CT anomalies (1948–70 climatology) and (b) the TI for all gauges in the region. (middle), (bottom) Difference of average CT for specified periods of the PDO: (c) the warm (1977–98) period minus the cool (1948–76) period and (d) the cool (1999–2002) period minus the warm (1977–98) period.

and PDO time series to the residual CT variations shows that temperature-dependent streamflow timing variations remain when PDO influences are removed, but not vice versa.

2) When the PDO influences on TI and CT variation are removed based on regression fits to the nontrending halves of the PDO series before and after 1976–77, much of the long-term timing trends in

most rivers of western North America remain. The 1976–77 PDO shift accounts for less than half of the observed streamflow timing trend in most western rivers, except in the Pacific Northwest.

3) The PDO appears to have shifted back to its cool phase in 1999 and remained in this phase until at least 2002. By contrast, the warming and earlier streamflow timing trends in western North America continued unabated, except for a comparatively small area in the Pacific Northwest and southwestern Canada, which historically has been most strongly connected to the PDO. The continuing early timing of snowmelt-driven streamflow is more similar to the continuing increases in greenhouse gas forcings and associated continued regional and global warming (TI and GSST) than to the 1999–2002 PDO reversal.

These findings indicate that the PDO is not sufficient to fully explain the observed CT and TI trends. In the Pacific Northwest, where PDO is most climatically influential on several time scales, the PDO's contribution to recent warming trends has been largest. But elsewhere, PDO typically has contributed less than half of the warming influences. Indeed, the best chance to discern the separate influences of PDO and greenhouse warming (or other causes) on the observed timing trends may be the most recent shift in PDO. The continuation of early streamflow timing despite a PDO reversal would argue for causes other than the PDO alone; however, four years (since the latest reversal) is not sufficient to determine confidently the mix of causes. Thus, continued attention to the trends described here and their continuing (or possibly diverging) relations to PDO will be necessary.

If observed streamflow timing trends persist, they will affect western water resources in several important ways. In western North America, springtime snowmelt has been relied upon to supply 50%–80% of the annual flow volume and is the most predictable part of the resource on season-to-season time scales. Progressively earlier snowmelt and snowfed streamflow will increasingly challenge many water resource management systems by modifying time-honored assumptions about the predictability and seasonal deliveries of snowmelt and runoff. Rivers where associated flood risks may change for the worse or where cool-season storage cannot accommodate lost snowpack reserves will likely be the most impacted. Earlier streamflow may impinge on the flood protection stages of reservoir operations so that less streamflow can be captured safely in key reservoirs. Almost everywhere in western North America, a 10%–50% decrease in the spring–summer streamflow fractions will accentuate the typical seasonal summer drought with important consequences for warm-season supplies, ecosystems, and wildfire risks. Together, these potential adverse consequences of the current trends heighten needs for continued and even enhanced monitoring of western snowmelt and runoff conditions and for incisive basin-specific assessments of the impacts to water supplies. A thorough determination of which basins will be impacted and a characterization of these impacts is needed to provide timely warnings of future changes and to foreshadow vulnerabilities of western water supplies and flood protection.

Acknowledgments. We gratefully acknowledge support for ITS through a UCAR/NOAA postdoctoral fellowship. Funding was provided by the DOE Office of Environmental Research, the NOAA Office of Global Programs through the California Applications Program, and the California Energy Commission through the California Climate Change Center. We thank Jon Eischeid and Henry Diaz for providing historical temperature and precipitation data and David Harvey of Environment Canada for supplying Canadian streamflow data. Mary Meyer Tyree provided invaluable data processing, analysis, and illustrations.

REFERENCES

Aguado, E., D. R. Cayan, L. G. Riddle, and M. Roos, 1992: Climatic fluctuations and the timing of West Coast streamflow. *J. Climate,* **5,** 1468–1483.

Bitz, C. M., and D. S. Battisti, 1999: Interannual to decadal variability in climate and the glacier mass balance in Washington, western Canada, and Alaska. *J. Climate,* **12,** 3181–3196.

Cayan, D. R., 1996: Interannual climate variability and snowpack in the western United States. *J. Climate,* **9,** 928–948.

——, K. T. Redmond, and L. G. Riddle, 1999: ENSO and hydrologic extremes in the western United States. *J. Climate,* **12,** 2881–2893.

——, S. A. Kammerdiener, M. D. Dettinger, J. M. Caprio, and D. H. Peterson, 2001: Changes in the onset of spring in the western United States. *Bull. Amer. Meteor. Soc.,* **82,** 399–415.

Dettinger, M. D., and D. R. Cayan, 1995: Large-scale atmospheric forcing of recent trends toward early snowmelt runoff in California. *J. Climate,* **8,** 606–623.

——, ——, H. F. Diaz, and D. M. Meko, 1998: North–south precipitation patterns in western North America on interannual-to-decadal timescales. *J. Climate,* **11,** 3095–3111.

——, ——, M. K. Meyer, and A. E. Jeton, 2004: Simulated hydrologic responses to climate variations and change in the Merced, Carson, and American River Basins, Sierra Nevada, California, 1900–2099. *Climatic Change,* **62,** 283–317.

Eischeid, J. K., C. B. Baker, T. R. Karl, and H. F. Diaz, 1995: The quality control of long-term climatological data using objective data analysis. *J. Appl. Meteor.,* **34,** 2787–2795.

Fountain, A. G., and W. V. Tangborn, 1985: The effect of glaciers on streamflow variations. *Water Resour. Res.,* **21,** 579–586.

Gleick, P. H., 1987: The development and testing of a water balance model for climate change impact assessment—Modeling the Sacramento Basin. *Water Resour. Res.,* **23,** 1049–1061.

Groisman, P. Y., and D. R. Easterling, 1994: Variability and trends of total precipitation and snowfall over the United States and Canada. *J. Climate,* **7,** 184–205.

——, T. R. Karl, R. W. Knight, and G. L. Stenchikov, 1994: Changes of snow cover, temperature, and radiative heat balance over the Northern Hemisphere. *J. Climate,* **7,** 1633–1656.

Hamlet, A. F., and D. P. Lettenmaier, 1999: Effects of climate change on hydrology and water resources in the Columbia River basin. *J. Amer. Water Resour. Assoc.,* **35,** 1597–1623.

Hodge, S. M., D. C. Trabant, R. M. Krimmel, T. A. Heinrichs, R.

S. March, and E. G. Josberger, 1998: Climate variations and changes in mass of three glaciers in western North America. *J. Climate,* **11,** 2161–2179.

Jeton, A. E., M. D. Dettinger, and J. L. Smith, 1996: Potential effects of climate change on streamflow, eastern and western slopes of the Sierra Nevada, California and Nevada. USGS Water Resources Investigations Rep. 95-4260, 44 pp.

Jones, P. D., T. J. Osborne, and K. R. Briffa, 2001: The evolution of climate over the last millennium. *Science*, **292,** 662–667.

Karl, T. R., P. Ya. Groisman, R. W. Knight, and R. R. Heim, 1993: Recent variations of snow cover and snowfall in North America and their relation to precipitation and temperature variations. *J. Climate,* **6,** 1327–1344.

Kim, J., 2001: A nested modeling study of elevation-dependent climate change signals in California induced by increased atmospheric CO_2. *Geophys. Res. Lett.,* **28,** 2951–2954.

Latif, M., and T. P. Barnett, 1994: Causes of decadal climate variability over the North Pacific and North America. *Science,* **266,** 634–637.

Lettenmaier, D. P., and T. Y. Gan, 1990: Hydrologic sensitivities of the Sacramento–San Joaquin River Basin, California, to global warming. *Water Resour. Res.,* **26,** 69–86.

——, E. F. Wood, and J. R. Wallis, 1994: Hydro-climatological trends in the continental United States, 1948–88. *J. Climate,* **7,** 586–607.

Livezey, R. E., M. Masutani, A. Leetmaa, H. Rui, M. Ji, and A. Kumar, 1997: Teleconnective response of the Pacific–North American region atmosphere to large central equatorial Pacific SST anomalies. *J. Climate,* **10,** 1787–1820.

Luckman, B. H., 1998: Landscape and climate change in the central Canadian Rockies during the 20th century. *Can. Geogr.,* **42,** 319–336.

——, K. R. Briffa, P. D. Jones, and F. H. Schweingruber, 1997: Tree-ring-based reconstruction of summer temperatures at the Columbia Icefield, Alberta, Canada, AD 1073–1983. *Holocene,* **7,** 375–389.

Mantua, N. J., S. R. Hare, Y. Zhang, J. M. Wallace, and R. C. Francis, 1997: A Pacific interdecadal climate oscillation with impacts on salmon production. *Bull. Amer. Meteor. Soc.,* **78,** 1069–1079.

McCabe, G. J., and A. G. Fountain, 1995: Relations between atmospheric circulation and mass balance of South Cascade Glacier, Washington, U.S.A. *Arct. Alp. Res.,* **7,** 226–233.

——, and M. D. Dettinger, 2002: Primary modes and predictability of year-to-year snowpack variations in the western United States from teleconnections with Pacific Ocean climate. *J. Hydrometeor.,* **3,** 13–25.

——, A. G. Fountain, and M. Dyurgerov, 2000: Variability in winter mass balance of Northern Hemisphere glaciers and relations with atmospheric circulation. *Arct. Antarct. Alp. Res.,* **32,** 64–72.

Miller, N., J. W. Kim, and M. D. Dettinger, 1999: California streamflow evaluation based on a dynamically downscaled 8-year hindcast (1988–1995), observations and physically based hydrologic models. *Eos, Trans. Amer. Geophys. Union* (Fall Meeting Suppl.), **80,** F406.

Mote, P. W., 2003a: Trends in snow water equivalent in the Pacific Northwest and their climatic causes. *Geophys. Res. Lett.,* **30,** 1601, doi:10.1029/2003GL017258.

——, 2003b: Trends in temperature and precipitation in the Pacific northwest during the twentieth century. *Northwest Sci.,* **77** (4), 271–282.

Namias, J., 1979: Premonitory signs of the 1978 break in the West Coast drought. *Mon. Wea. Rev.,* **107,** 1675–1681.

NCEP, cited 2003: Monthly atmospheric and SST indices. [Available online at http://www.cpc.ncep.noaa.gov/data/indices/.]

Pupacko, A., 1993: Variations in Northern Sierra Nevada streamflow: Implications of climate change. *Water Resour. Bull.,* **29,** 283–290.

Redmond, K. T., and R. W. Koch, 1991: Surface climate and streamflow variability in the Western United States and their relationship to large-scale circulation indexes. *Water Resour. Res.,* **27,** 2381–2399.

Regonda, S. K., B. Rajagopalan, M. Clark, and J. Pitlick, 2005: Seasonal cycle shifts in hydroclimatology over the western United States. *J. Climate,* **18,** 372–384.

Roos, M., 1987: Possible changes in California snowmelt patterns. *Proc. Fourth Pacific Climate Workshop*, Pacific Grove, CA, PACLIM, 22–31.

——, 1991: A trend of decreasing snowmelt runoff in Northern California. *Proc. 59th Western Snow Conf.*, Juneau, AK, Western Snow Conference, 29–36.

Ropelewski, C. F., and M. S. Halpert, 1986: North American precipitation and temperature patterns associated with the El Niño/Southern Oscillation (ENSO). *Mon. Wea. Rev.,* **114,** 2352–2362.

Slack, J. R., and J. M. Landwehr, 1992: Hydro-Climatic Data network (HCDN): A U.S. Geological Survey streamflow data set for the United States for the study of climate variations, 1874–1988. U.S. Geological Survey Open-File Rep. 92-129, 193 pp.

Snyder, M. A., J. L. Bell, L. C. Sloan, P. B. Duffy, and B. Govindasamy, 2002: Climate responses to a doubling of atmospheric carbon dioxide for a climatically vulnerable region. *Geophys. Res. Lett.,* **29,** 1514, doi:10.1029/2001GL014431.

Stewart, I. T., D. R. Cayan, and M. D. Dettinger, 2004: Changes in snowmelt runoff timing in western North America under a "business as usual" climate change scenario. *Climatic Change,* **62,** 217–232.

Trenberth, K. E., 1996: Coupled climate systems modeling. *Climate Change: Developing Southern Hemisphere Perspectives,* T. W. Giambelluca and A. Henderson-Sellers, Eds., John Wiley & Sons, 63–88.

Vincent, L. A., X. Zhang, and W. D. Hogg, 1999: Maximum and minimum temperature trends in Canada for 1895–1995 and 1946–1995. Preprints, *10th Symp. on Global Change Studies*, Dallas, TX, Amer. Meteor. Soc., 95–98.

Wahl, K. L., 1992: Evaluation of trends in runoff in the western United States. *Managing Water Resources during Global Change: AWRA 28th Annual Conference & Symposium: An International Conference, Reno, Nevada, November 1–5, 1992,* R. Herrmann, Ed., Technical Publication Series, Vol. 92-4, American Water Resources Association, 701–710.

Walters, R. A., and M. F. Meier, 1989: Variability of glacier mass balances in western North America. *Aspects of Climate Variability in the Pacific and the Western Americas*, *Geophys. Monogr.*, No. 55, Amer. Geophys. Union, 365–374.